Proceedings of the
International Conference on Mechanical Engineering and Renewable Energy 2011
(ICMERE2011) 22- 24 December 2011, Chittagong, Bangladesh
ICMERE2011-PI-044

MARTENSITIC TRANSFORMATION IN BULK Ni-Mn-Sn ALLOYS

M. Nazmunnahar[1*], M. Ilyn[1], L. González[2], J. García[2], J.J. del Val[1], M.L Sánchez[2], J.D. Santos[2], V.M. Prida[2], V. Koledov[3], B. Hernando[2], J. González[1]

[1] Material Physics Dept., Chemistry Fac., Basque Country University, 1072, 20080-San Sebastián, Spain.
[2] Departamento de Física, Universidad de Oviedo, Calvo Sotelo s/n, 33007-Oviedo, Spain.
[3] Kotelnikov Institute of Radio Engineering and Electronics, RAS, Moscow 125009, Russia.
* Corresponding author:nazu_duet@yahoo.com

Abstract

In this report we show the structural and magnetic properties on bulk polycrystalline ingot, which nominal compositions $Ni_{50}Mn_{38}Sn_{12}$. This Heusler alloy was investigated by differential scanning calorymetry measurement (DSC) and the vibrating sample magnetometry technique (VSM). These measurements confirm the austenite-martensite structural transformation in the temperature range from 5 K up to 350 K. The start and finish temperatures of the martensitic phase transformation were M_s = 208 K and M_f = 181 K, while the ones found for austenite were A_s = 192 K and A_f = 221 K. The Curie temperature for the austenite is around 298 K. The complex behaviour exhibited by this Heusler alloy could be due to the strong coupling between magnetism and structure, and its magnetic behaviour strongly depends on the distance between Mn atoms.

Keywords:Martensitic transformation, Martensite start, Martensite finish, Heusler alloy, Magnetocaloric effect.

1. INTRODUCTION

Ni-Mn-*X* (*X*=Ga, Sb, In, Sn) Heusler alloy systems have attracted much attention thanks to their potential applications in magnetic refrigeration, magnetic actuated devices and spintronic devices [1-2]. By tuning the composition, this alloy system exhibits a wide range of physical properties such as magnetic-field-induced transition, inverse magnetocaloric effect (IMCE), giant magnetoresistance, giant Hall effect, giant magnetothermal conductivity, magnetic superelasticity effects, exchange bias and shape memory effect [3-8]. The complex behaviour exhibited by this non-stoichiometric Ni-Mn-Sn Heusler alloy is due to the strong coupling between magnetism and structure, and also the magnetic behaviour of these alloys strongly depends on the distance between Mn atoms [9]. However, the Ni-Mn-Sn alloy system is particularly an interesting class of materials because of the large reported IMCE [10]. The structural and magnetic properties of these alloys are very sensitive to the composition [11]. A specific feature of these alloys is that the saturation magnetization is greatly reduced or becomes almost zero upon the structural transformation from austenite to martensite [12-17]. It has been reported that in $Ni_{50}Mn_{25+x}Z_{25-x}$ (Z=Sn, In, Sb), the origin of this alloys was suggested to be the strengthening of antiferromagnetic interactions caused by an abrupt change in the Mn-Mn inter-atomic distances occurring upon the martensite transformation [18].

Recently, in Ga free $Ni_{50}Mn_{50-y}X_y$ (X=In, Sn and Sb) series of Heusler alloys, positive magnetic entropy change (ΔS_M) often termed as inverse MC effect (IMCE) has been reported in the vicinity of the first order structural transformation (FOST) due to the strong coupling between magnetism and structure [19-21]. It has been reported that the transformation takes place from the cubic $L2_1$ structure (Fm3m) to an orthorhombic four layered (4O) structure (Pmma) [13, 22]. Moreover, the studies reveal that in $Ni_{50}Mn_{37}Sn_{13}$ alloys, the Curie temperature (T_c), the martensite start (M_s) and the austenite finish (A_f) temperatures have occurred close to room temperature [18]. S. Esakki Muthu et al. [11] have been reported that the effect of varying Ni/Mn or Mn/Sn content on the structural and magnetic transformations in $Ni_{50-x}Mn_{37+x}Sn_{13}$ (x=0, 1, 2, 3, 4) alloys, the structural transition temperature was found to be the same. It has also been reported that the increase in Mn concentration decrease the martensite transition temperature. However, this suggests that the structural transformation is governed mainly by the e/a ratio in these alloys.

In addition, ferromagnetic shape memory alloys exhibit ferromagnetic and shape effect simultaneously. The ferromagnetic shape effect can be controlled by temperature and stress, as well as by magnetic field. Their potential functional properties are: magnetic superelasticty [23], large inverse magnetocaloric effect [24], and large magneto-resistance change [25]. Shape memory alloys exhibit a martensite phase transition. This transformation is a first order phase transition which takes place by the diffusion less shearing of the parent austenitic phase. By lowering the temperature a cubic high temperature parent austenite phase transforms into a tetragonal, orthorhombic, or monoclinic martensite ordered by domains. Thermal analysis is useful to determine transformation temperatures in ferromagnetic alloys with structural transformations [26-27]. The transformation temperatures of shape memory alloys strongly depend on the composition and their values spread in a very wide range [28].

Sutou et al. [18] first reported the martensitic transformation in ferromagnetic Heusler $Ni_{50}Mn_{50-x}Sn_x$ alloys with $10 \leq x \leq 16.5$. Later, Krenke et al. studied phase transformations, magnetic and magnetocaloric properties of the Heusler $Ni_{50}Mn_{50-x}Sn_x$ alloy series with $5 \leq x \leq 25$. Koyama et al. [22], Brown et al. [13] reported on the structural and magnetoelastic behavior of the alloy $Ni_{50}Mn_{36}Sn_{14}$. This alloy exhibits a large negative magneto-resistance effect accompanied by the magnetic-field induced reverse transformation. However, Santos et al. have been reported that in $Ni_{50}Mn_{37}Sn_{13}$ alloy, at low temperature, the ferromagnetic austenite phase transforms into a seven layered orthorhombic martensite phase [29]. Han et al. have investigated the magnetocaloric effect in $Ni_{50-x}Mn_{39-x}Sn_{11}$(x=5, 6, 7) near martensitic transition [21]. Therefore, Ni-Mn-Sn system is of prospective importance as ferromagnetic shape memory alloy and promising magnetic refrigerant alloy. In the present work, we have investigated Ni-Mn-Sn based sample with bulk $Ni_{50}Mn_{38}Sn_{12}$ composition in order to develop materials with a martensite transformation around room temperature.

2. EXPERIMENTAL

The master alloy $Ni_{50}Mn_{38}Sn_{12}$ was produced by arc-melting, employing highly pure elements. The obtained ingots were annealed in evacuated quartz capsule for 24 h at 1173K and subsequently cooled down at room temperature. The ingot was cut in small pieces by low speed diamond saw. The crystal structure was determined by X-ray diffraction (XRD) using CuKα radiation at room temperature and the microstructure of the bulk, as well as the compositions, were performed through Scanning Electron Microscopy (SEM, JEOL 6100) equipped with an Energy Dispersive X-ray microanalysis system (EDX, Inca Energy 200). Differential Scanning Calorimetry (DSC) measurements below room temperature was carried out in the DSC Q 2000 calorimeter with a liquid nitrogen cooling system in a heating and cooling rate of 5K/min. The magnetic properties were measured on bulk by Vibrating Sample Magnetometry (VSM, Quantum Desing Versalab) in the temperature range of 5–350 K and up to 3 T applied field. MT was characterized from the thermomagnetic measurements, which means zero-field cooling (ZFC), field cooling (FC) and field heating (FH) routines that were performed using different applied magnetic fields. The heating and cooling rates were of 5 K/min.

3. RESULTS AND DISCUSSION

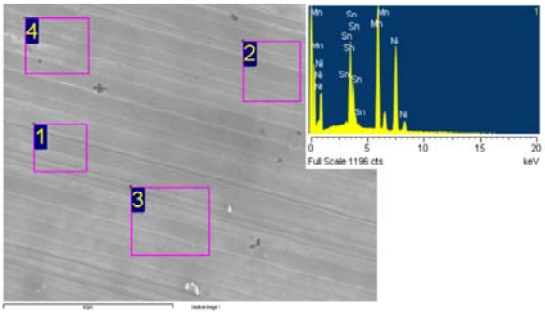

FiG.1.(Color online) SEM micrograph of the different regions $Ni_{50}Mn_{38}Sn_{12}$ bulk alloy.Inset:Typical EDS spectrum.

SEM/EDX microanalysis for Ni-Mn-Sn sample an averaged composition of $Ni_{44.2}Mn_{42.28}Sn_{13.50}$ has found after a careful study carried out at different points of the sample. Segregation of minor or secondary phases was not observed.It is observed an appreciable shift of the nominal composition, which could cause changes in the magnetic properties with respect to this one.

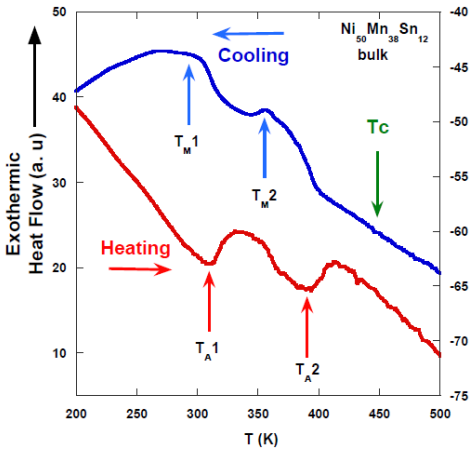

Figure 2: DSC cycles scans for the alloy $Ni_{50}Mn_{38}Sn_{12}$ at heating and cooling rate of 5K/min.

Fig.2 shows the DSC heating and cooling curves in $Ni_{50}Mn_{38}Sn_{12}$. A broad exothermic (endothermic) peak, corresponding to an austenite (martensitic) transformation at heating (cooling) curve, are observed in the

temperature range 300 K and 360 K. The characteristic transition temperatures are T_A^1 = 314 K, T_A^2 = 365 K, T_M^1 = 300 K and T_M^2 = 355 K. At higher temperatures, small exothermic peak is detected on heating. It corresponds to the Curie temperature of the austenite phase (T_c).Its denoting that the re-crystallization process is very complex. This complexity is supported by the XRD results, whose scan for bulk sample is shown in Fig. 3. XRD pattern show the presence of, mainly, Ni, Mn and cubic Ni_2MnSn crystalline L_{21} phases and an overlapping amorphous halo which can be attributed to a high quantity of amorphous still non crystallized. Therefore, we can say that the re-crystallized sample is formed by multiple crystalline phases. It is important to point out that 5 and 6 nm sizes were obtained for Ni_2MnSn crystals, from Scherer's formula [34] after correction of the experimental broadening with a big crystallite standard.

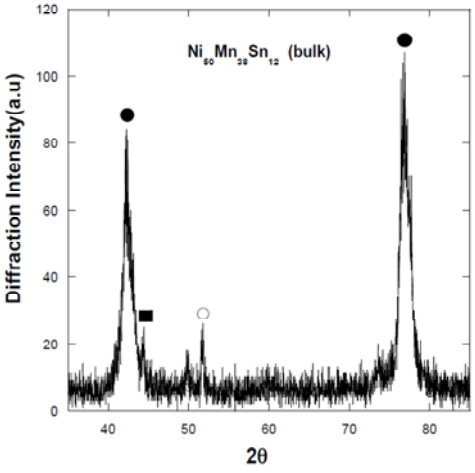

Fig: 3. XRD scans obtained at RT for $Ni_{50}Mn_{38}Sn_{12}$bulk alloy. Ni (○), Mn (■), and Ni_2MnSn (●) peaks have been signaled.

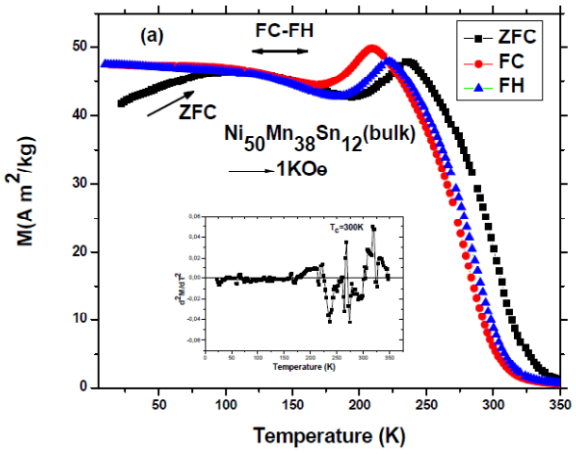

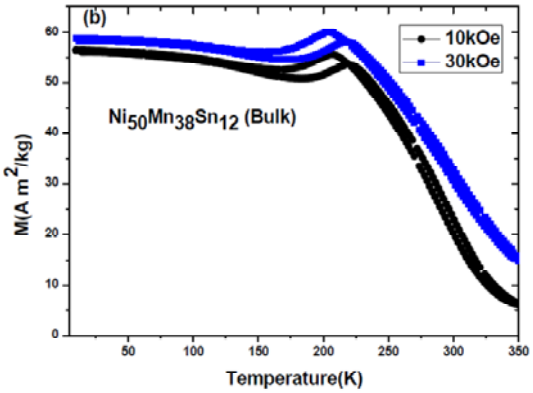

Figure 4: Temperature dependence of magnetization measured at (a) H = 1 kOe and (b) H = 10 kOe and H = 30 kOe for $Ni_{50}Mn_{38}Sn_{12}$ alloy. Inset of (a) d^2M/dT^2 curve at 1kOe.

Figure 4 (a) shows the thermo-magnetization curves on cooling and heating obtained by the VSM technique for $Ni_{50}Mn_{38}Sn_{12}$ alloy at a magnetic field strength of H = 1kOe. The thermo-magnetization curves first increase due to the magnetic transformation from the paramagnetic to the ferromagnetic state in the cooling stage from around 298 K. The T_c temperature, which is defined as the temperature at which the slope of magnetization versus temperature curve is the largest, has been calculated from the inflection point of the second derivate with the X-axis (see inset). Subsequently, the magnetization decreases due to the martensitic transformation. This phenomenon is in good agreement with those obtained by the DSC which suggests the existence of the martensite-austenite transformation. Moreover, It can be clearly seen that the FH and FC curves do not trace the same path but display thermal hysteresis (ΔT = 11 K) which is the signature of FOST. The structural transformation shows the start and finish temperatures of the martensitic phase transformation of M_s = 208 K and M_f = 181 K, while the ones found for austenite is A_s = 192 K and A_f = 221 K, in agreement with previously reported values in similar compositions [30]. The complex behavior exhibited by this non-stoichiometric Heusler alloy is due to the strong coupling between magnetism and structure, and its magnetic behavior strongly depends on the distance between Mn atoms.

In Fig.4 (b) it is observed that when increasing the applied magnetic field the magnetic moment suffers a drastically increase and the structural transformation is shifted to smaller temperatures than the other ones at low field, see Fig.4 (a). An similar behavior has been found earlier in Ni-Mn-Sn ribbons of similar compositions [31]. The abrupt change of MT, around crystal transition temperatures, suggests a significant and positive magnetic entropy change ΔS_M associated with an inverse

magnetocaloric effect. Ferromagnetic behavior for the sample with H = 30 kOe is observed in austenitic state below $T_c^A \sim 312K$ but further decrease in the temperature causes a sudden decrease in the magnetization below MT and is in fact, comparable to the one found in bulk materials of $Ni_{50}Mn_{36}Sn_{14}$ composition [32]. At high temperature, the sample is in the austenite state and orders ferromagnetically below 312 K. However, below the M_s Temperature, sample exhibits a decrease in the magnetization which reaches to a minimum as the proportion of the ferromagnetic austenite phase progressively decreases (Fig.4 (b)). The same behavior has been reported in melt spun $Ni_{49}Mn_{37.4}Sn_{13.6}$ ribbon [33].

4. CONCLUSION

In conclusion, a martensitic transformation temperature of $Ni_{50}Mn_{38}Sn_{12}$ bulk alloy have been detected at 208 K for martensitic phase starting meanwhile the corresponding finishing temperature is achieved at 181 K for it. Thermomagnetic measurements for different values of the applied magnetic field revealed that characteristic transformations temperatures decrease with the field increasing from 1kOe to 30kOe. The increment in magnetization around structural transition, points to the fact that the Heusler alloy here studied could be of potential interest in multifunctional applications such as actuator and or magnetocaloric material. More work with these purposes is now in progress.

5. ACKNOWLEDGEMENTS

Authors are thankful to Spanish MICINN for financial support: MAT2009-13108-C02-01-02 and MAT2010-20798-C05-04. M.Nazmunnahar thanks to Basque government for a grant. L. González also thanks to MICINN for a FPI grant and J. García to FICYT for a "Severo Ochoa" grant.

6. REFERENCES

[1] Planes A., Mañosa L., Acet M. *J., Phys.: Condens. Matter* **21**, (2009) 233201.
[2] Cong D. Y., Roth S., Pötschke M., Hürrich C., Schultz L., *Appl. Phys. Lett.* **97**, (2010) 021908.
[3] Rama Rao N. V., Gopalan R., Chandrasekaran V., Suresh K. G., *Appl. Phys. A. Mater. Sci. Process.* **99**, (2010) 265.
[4] Yu S. Y., Liu Z. H., Liu G. D., Chen J. L., Cao Z. X., Wu G. H., Zhang B., Zhang X., *Appl. Phys. Lett.* **89**, (2006) 162503.
[5] Biswas C., Rawat R., Barman S. R., *Appl. Phys. Lett.* **86**, (2005) 202508.
[6] Oikawa K., Ito W., Imano Y., Sutou Y., Kainuma R., Ishida K., Okamoto S., Kitakami O., Kanomata T., *Appl. Phys. Lett.* **88**, (2006) 122507.
[7] Sozinov A., Likhachev A. A., Lanska N., Ullakko K., *Appl. Phys. Lett.* **80**, (2002) 1746.
[8] Hu F. X., Shen B. G., Sun J. R., *Appl. Phys. Lett.* **76**, (2000) 3460.
[9] Planes A., *Physics* **3**, (2010) 36.
[10] Krenke T., Duman E., Acet M., Wassermann E. F., Moya X., Mañosa L., Planes A., *Nature Mater.* **4**, (2005) 450.
[11] Esakki S. Muthu, Rama Rao N. V., Manivel Raja M., Raj Kumar D. M., Mohan Radheep D., Arumugam S., *J. Phys. D: Appl. Phys.* **43**, (2010) 425002.
[12]. Krenke T., Acet M., Wassermann E. F., Moya X., Mañosa L., Planes A., *Phys. Rev. B* **72**, (2005) 014412.
[13] Brown P. J., Gandy A. P., Ishida K., Kainuma R., Kanomata T., Neumann K.U., Oikawa K., Ouladdiaf B., Ziebeck K. R. A., *J. Phys.: Condens. Matter* **18**, (2006) 2249.
[14] Kainuma R., Imano Y., Ito W., Morito H., Sutou Y., Oikawa K., Fujita A., Ishida K., Okamoto S., Kitakami O., Kanomata T., *Appl. Phys. Lett.* **88**, (2006) 192513.
[15] Krenke T., Acet M., Wassermann E. F., Moya X., Mañosa L., Planes A., *Phys. Rev. B* **73**, (2006) 174413.
[16] Khan M., Dubenko I., Stadler S., Ali N., *J. Phys.: Condens. Matter* **20**, (2008) 235204.
[17] Khovaylo V. V., Skokov K. P., Gutfleisch O., Miki H., Takagi T., Kanomata T., Koledov V. V., Shavrov V.V., Wang G., Palacios E., Bartolomé J., Burriel R., *Phys. Rev. B* **81**, (2010) 214406.
[18] Sutou Y., Imano Y., Koeda N., Omori T., Kainuma R., Ishida K., Oikawa K., *Appl. Phys. Lett.* **85** (2004) 4358.
[19] Bruck E. *J., Phys. D: Appl. Phys*. **38** (2005) R381.
[20] Han Z. D., Wang D. H., Zhang C. L., Tang S. L., Gu B. X., Du Y. W., *Appl. Phys. Lett*. **89**, (2006) 182507.
[21] Han Z. D., Wang D. H., Zhang C. L., Xuan H. C., Gu B. X., Du Y. W., *Appl. Phys. Lett.* **90**, (2007) 042507.
[22] Koyama K., Watanabe K., Kanomata T., Kainuma R., Oikawa K., Ishida K., *Appl. Phys. Lett.* **88**, (2006) 132505.
[23] Krenke T., Duman E., Acet M., Wassermann E. F., Moya X., Mañosa L., *Phys Rev B.* **7575**, (2007) 104414.
[24] Pons J., Chernenko V. A., Santamarta R., Cesari E., *Acta Mater.* **48**, (2000) 3027–3038.
[25] Koike K., Ohtsuka M., Honda Y., Katsuyama H., Matsumoto M., Itagaki K., *J Magn Magn Mater.*; **310** (2007) 996–998.
[26] Bonastre J., Escoda L., González A., Saurina J., Suñol J. J., *J. Therm. Anal. Calorim.*; **88**, (2007) 83–86.
[27] González A., Bonastre J., Escoda L., Suñol J. J., *J. Therm. Anal. Calorim.;* **87**, (2007) 255–258.
[28] Bhobe P. A., Priolkar K. R., Nigam A. K., *Appl Phys Lett.;* **91**, (2007) 242503.
[29] Santos J. D., Sanchez T., Alvarez P., Sanchez M. L., Sánchez Llamazares J. L., Hernando B., *J. Appl. Phys.* **103**, (2008) 07B326.

[30] Coll R., Escoda L., Saurina J., Sánchez Llamazares J.L., Hernando B., Suñol J. J, *J., Therm. Anal. Calorim*. **99**, (2010) 905–909.
[31] Hernando B., Sánchez Llamazares J. L., Santos J. D., Escoda LI., Suñol J. J., Varga R., Baldomir D., Serantes D., *App. Phy. Let* **92**, (2008) 042504.
[32] Dubowik J., Szlaferek A., Gosciannska I., *Acta. Phy. Polonica A*, **113** (2008).
[33] Babita I., Patil S. I., Ram S.; *J. Phys. D: Appl. Phys.* **43** (2010) 205002
[34] H. P. Klug and L. E. Alexander, *X-ray diffraction procedures for polycrystalline and amorphous materials*, Wiley, New York (1974).

7. NOMENCLATURE

Symbol	Meaning	Unit
T	Temperature	(K)
M	Magnetization	(A m^2/kg)
H	Magnetic field	(A/m)
T_c	Curie temperature	(K)